Electron-transfer activation of the aminocarbyne and the hydrogen isocyanide complexes trans-$[ReCl(CNH_n)(Ph_2PCH_2CH_2PPh_2)_2][BF_4]_{n-1}$ ($n=2$ or 1). Interconversion of coordinated CNH_2 and CNH

M. Amélia N.D.A. Lemos, M. Fátima C. Guedes da Silva, Armando J.L. Pombeiro *

Centro de Química Estrutural, Complexo I, Instituto Superior Técnico, Av. Rovisco Pais, 1096 Lisbon Codex, Portugal

Abstract

The aminocarbyne complex trans-$[ReCl(CNH_2)(dppe)_2][BF_4]$ (dppe = $Ph_2PCH_2CH_2PPh_2$) undergoes, by cyclic voltammetry in 0.2 M $[NBu_4][BF_4]$/NCMe, at a Pt electrode, a single-electron oxidation involving anodically induced deprotonation to give the hydrogen isocyanide compound trans-$[ReCl(CNH)(dppe)_2]^+$ which exhibits, at a higher potential, a similar anodic process. Both trans-$[ReCl(CNH_2)(dppe)_2][BF_4]$ and trans-$[ReCl(CNH)(dppe)_2]$ can undergo proton dissociation in solution and, by cathodic reduction, dihydrogen is evolved with conceivable formation of cyanide species. The mechanism of the anodic processes has been investigated by digital simulation of cyclic voltammograms which allowed the rate constants of the deprotonation reactions induced by electron transfer, and the acid dissociation constants for the aminocarbyne species and its oxidized form, to be estimated.

Keywords: Electron transfer activation; Rhenium complexes; Aminocarbyne complexes; Hydrogen isocyanide complexes; Electrochemistry

1. Introduction

In contrast with the developed chemistry of complexes with multiple metal–carbon bonded species [1], only a very limited number of studies, although rather promising, have been reported on their electrochemical behaviour, namely involving redox-induced rearrangement [2], coupling [2], insertion [3] or protonation [4] reactions of vinylidenes, conformation changes of carbenes [5], deprotonation of aminocarbenes [6], dehydrogenation of carbynes or η^2-vinyls [7], or dioxocarbene cleavage [8].

The present work focuses on the electrochemical behaviour of the aminocarbyne complex trans-$[ReCl(CNH_2)(dppe)_2][BF_4]$ (dppe = $Ph_2PCH_2CH_2$-PPh_2) and follows a preliminary account [7]. When reported, it provided the first example of a complex with the simplest aminocarbyne species (CNH_2) stabilized by coordination, and was prepared [9] by reaction of HBF_4 with trans-$[ReCl(CNSiMe_3)(dppe)_2]$ (upon N–Si bond cleavage with formation of Me_3SiF). How-

ever, it can also be obtained by protonation of the corresponding hydrogen isocyanide compound trans-$[ReCl(CNH)(dppe)_2]$.

The anodic behaviour of the other known mononuclear CNH_2 complexes, the related molybdenum or tungsten compounds trans-$[MCl(CNH_2)(dppe)_2]$ (M = Mo [10a] or W [10b]), electrosynthesized from trans-$[MCl(CN)(dppe)_2]$ (by a $2e^-/2H^+$ process), has been reported and shown to involve the inverse overall $-2e^-/-2H^+$ process to regenerate the parent cyanide complexes. However, no mechanistic study was reported.

As discussed below, our work, which also includes a mechanistic investigation, establishes the ready electro-induced conversion of CNH_2 into CNH at an Re centre and presents evidence for the involvement of the latter group in the CNH_2/CN^- interconversion.

The coordination chemistry of those species may be of particular significance for obtaining an insight into the mechanism of the reduction of aqueous cyanide to methylamine, methane and ammonia by nitrogenase [11].

Moreover, CNH has been detected in the interstellar space [12] and CNH_2^+ is also believed [13] to exist

therein and to be an important precursor for the interstellar synthesis of CNH and NCH, in particular by the postulated dissociate recombination $CNH_2^+ + e^-$, a reaction we have attempted in this work, although by electrochemical methods, for the metal-stabilized CNH_2^+ ligand. Therefore, it is not surprising that the gas phase ion chemistry [13c] of such species is receiving considerable attention and the recent growth of interest [14] on the emergence of a CNH and cyano based organometallic chemistry is also noteworthy.

2. Experimental

The complexes *trans*-[ReCl(CNH_2)(dppe)_2][BF_4] and *trans*-[ReCl(CNH)(dppe)_2] were prepared according to published procedures [9] and the solvents were dried and degassed by using standard techniques.

The electrochemical experiments were carried out either on an EG&G PAR 173 potentiostat/galvanostat and an EG&G PARC 175 Universal programmer or on an HI-TEK DT 2101 potentiostat/galvanostat and an HI-TEK PP RI waveform generator. Cyclic voltammetry was undertaken in a two-compartment three-electrode cell, at a platinum wire or disc or a vitreous carbon working electrode, probed by a Luggin capillary connected to a silver-wire pseudo-reference electrode; a platinum or tungsten auxiliary electrode was employed. Controlled-potential electrolysis were carried out in a three-electrode H-type cell with platinum-gauze working and counter electrodes in compartments separated by a glass frit; a Luggin capillary, probing the working electrode, was connected to a silver-wire pseudo-reference electrode. The oxidation potentials of the complexes were measured by cyclic voltammetry in 0.2 mol dm^{-3} [NBu_4][BF_4]/NCMe and the redox potential values are quoted relative to the SCE by using as internal reference the [Fe(η^5-C_5H_5)_2]^{0/+} couple ($E_{1/2}^{ox} = 0.55$ V versus SCE, in 0.2 mol dm^{-3} [NBu_4][BF_4]/NCMe).

The acid–base potentiometric titrations of the electrochemically oxidized solutions were carried out by using a solution of NaOH in MeOH which was standardized by titration against benzoic acid in NCMe. The results presented have been corrected for background effects by performing also, in each case, the titration of the blank solution of 0.2 mol dm^{-3} [NBu_4][BF_4] which has been electrolyzed under identical conditions to those used for the corresponding complex solution.

Moreover, prior to the addition of the complex, each electrolyte solution was pre-electrolyzed at the appropriate potential until a constant and close to zero current, thus conceivably eliminating the interference of eventual traces of residual moisture during the subsequent controlled-potential electrolysis of the complex solution.

The digital simulation was carried out using a program developed in Turbo Pascal Version 6 (© Borland International). The relevant partial differential equations were solved by the 'method of lines', using a non-uniform space grid for the space discretization process. This grid uses an exponentially expanding space element

$$\Delta x_i = \Delta x_0 \exp(\beta i) \quad i = 0, 1, \ldots, n$$

as proposed by Joslin and Pletcher [15] for the finite differences method and applied to the 'method of lines' in a previous work [16]. The expansion parameter (β) used in these simulations was 0.1, and the width of the first element (Δx_0) was adjusted so that the total extension of the diffusion layer used in the computations met the estimation made, for each individual voltammogram, according to Ref. [17].

The integration of the ordinary differential equations obtained after space discretization was performed by the fourth order Runge–Kutta method, which was demonstrated to be a suitable numerical integration scheme for cyclic voltammetry problems, concerning stability, computation time and error, as discussed previously [18].

For simulation purposes, the experimental cyclic voltammograms were base-line corrected for comparison with the theoretical ones. The diffusion coefficient (D) for the complexes was estimated as $\sim 1 \times 10^{-5}$ cm² s⁻¹, by comparison between their current-function and that of ferrocene which is known [19] to present $D = 2.15 \times 10^{-5}$ cm² s⁻¹. The transfer coefficient (α) was assumed to be 0.5 in all cases.

The program was run on a 486DX2/66 MHz based IBM compatible personal computer.

The gas chromatographic analysis were performed with a Shimadzu GC4P gas chromatograph equipped with a Shimadzu CR3A integrator, a 13 X molecular sieve packed column and a TCD detector. Helium was used as the carrier gas.

3. Results and discussion

3.1. Anodic behaviour

The cyclic voltammograms of a 0.2 M [NBu_4][BF_4]/NCMe solution of the aminocarbyne complex *trans*-[ReCl(CNH_2)(dppe)_2][BF_4], denoted onwards, in a simplified way, by $Re(CNH_2)^+$ (where Re stands for the metal site *trans*-{ReCl(dppe)_2}), presents a first irreversible anodic wave (wave I) at $^IE_{p/2}^{ox} = 0.90$ V versus SCE (the quoted redox potential values were measured at 200 mV s⁻¹) which is followed, at a higher potential ($^{II}E_{p/2}^{ox} = 1.63$ V), by a second, and also irreversible, anodic process (wave II) (Figs. 1 and 2). They appear to involve a single-electron transfer, as indicated by
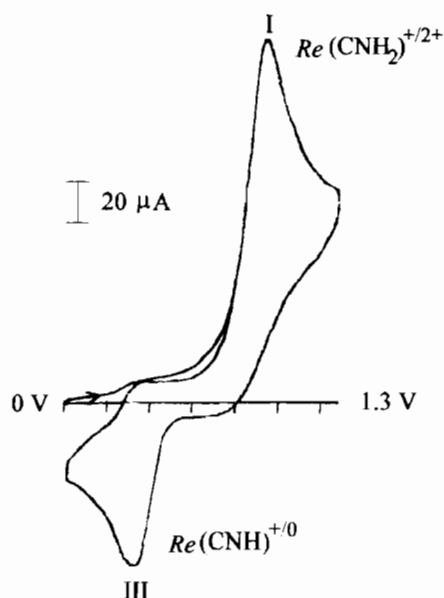
Fig. 1. Cyclic voltammograms (up to the first anodic wave I) for a solution of *trans*-[ReCl(CNH$_2$)(dppe)$_2$][BF$_4$] (0.99 mmol dm^{-3}) in 0.2 mol dm^{-3} [NBu$_4$][BF$_4$]/NCMe, at a Pt wire electrode (scan rate = 500 mV s^{-1}; potential in V vs. SCE). Wave III corresponds to the reduction of *Re*(CNH)$^+$ generated at wave I. *Re* = *trans*-{ReCl(dppe)$_2$}.

comparison of their current-functions with that of the one-electron anodic wave of *trans*-[ReCl(N$_2$)(dppe)$_2$]; moreover, the current-functions do not vary substantially with the scan rate (at least for scan rates in the range of ~50–1000 mV s^{-1}).

3.1.1. First anodic wave

The anodic process at wave I generates the mono-oxidized form of the known hydrogen isocyanide complex *trans*-[ReCl(CNH)(dppe)$_2$], i.e. *Re*(CNH)$^+$ (Eq. (1)) derived from proton loss of the oxidized aminocarbyne complex, on the basis of the following evidence:

$$Re(CNH_2)^+ \underset{-e^-}{\overset{(I)}{\rightleftharpoons}} Re(CNH_2)^{2+} \longrightarrow$$

$$Re(CNH)^+ + H^+ \quad (1)$$
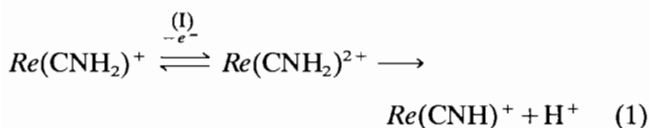
(i) The product of the single-electron oxidation presents the expected cyclic voltammetric behaviour (Figs. 2 and 3) for *Re*(CNH)$^+$, being reduct (wave III) and oxidized (wave II) at potentials ($E_{p/2}^{red} = 0.42$ V and $E_{p/2}^{ox} = 1.63$ V, respectively) which are identical to those corresponding to the redox pairs *Re*(CNH)$^{0/+}$ and *Re*(CNH)$^{+/2+}$, respectively, derived from a genuine sample of *Re*(CNH) (see below). Moreover, the oxidation at $E_{p/2}^{ox} = 1.63$ V (wave II) generates a species (for its identification, see below) which is reduced at $E_{1/2}^{red} = 1.20$ V (wave IV) (Fig. 2), as observed for the second anodic process of *Re*(CNH), i.e. that product is formed from *Re*(CNH)$^{2+}$.
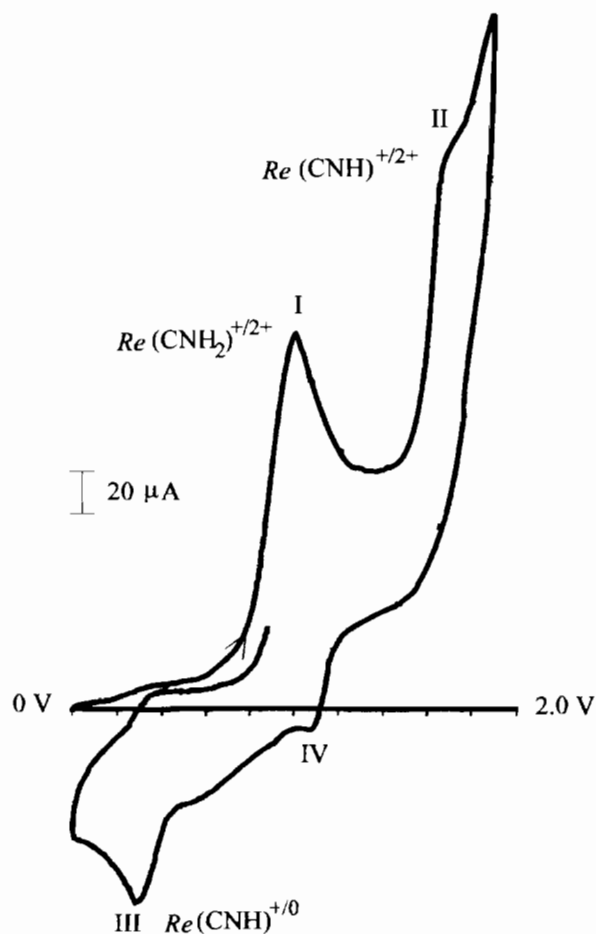

Fig. 2. Cyclic voltammogram (extended to the second anodic wave II) for a solution of *trans*-[ReCl(CNH$_2$)(dppe)$_2$][BF$_4$] (0.99 mmol dm^{-3}), in 0.2 mol dm^{-3} [NBu$_4$][BF$_4$]/NCMe, at a Pt wire electrode (scan rate = 500 mV s^{-1}; potential in V vs. SCE). Waves II and III correspond to the oxidation and reduction, respectively, of *Re*(CNH)$^+$ generated at wave I. Wave IV is due to the reduction of postulated *Re*(CN)$^+$ derived from *Re*(CNH)$^{2+}$ generated at wave II. *Re* = *trans*-{ReCl(dppe)$_2$}.

In fact, under identical cyclic voltammetric experimental conditions, the hydrogen isocyanide complex *Re*(CNH), independently prepared by methanolysis of *trans*-[ReCl(CNSiMe$_3$(dppe)$_2$] [9], presents a first single-electron reversible oxidation at $E_{1/2} = 0.40$ V which is followed, at a higher potential ($E_{p/2}^{ox} = 1.63$ V) by a single-electron irreversible anodic process which forms a new species with a reversible reduction wave at $E_{1/2}^{red} = 1.20$ V, in agreement with the behaviour described above for the product of the monooxidation of *Re*(CNH$_2$)$^+$.

However, the cathodic wave of *Re*(CNH)$^+$ (wave III), formed at the anodic process of *Re*(CNH$_2$)$^+$ (Eq. (1)), is not reversible, in contrast with the reversible character of the redox wave for the couple *Re*(CNH)$^{0/+}$ when obtained from a genuine sample of pure *Re*(CNH). That irreversibility results from the presence, in the former case, of free H$^+$, liberated
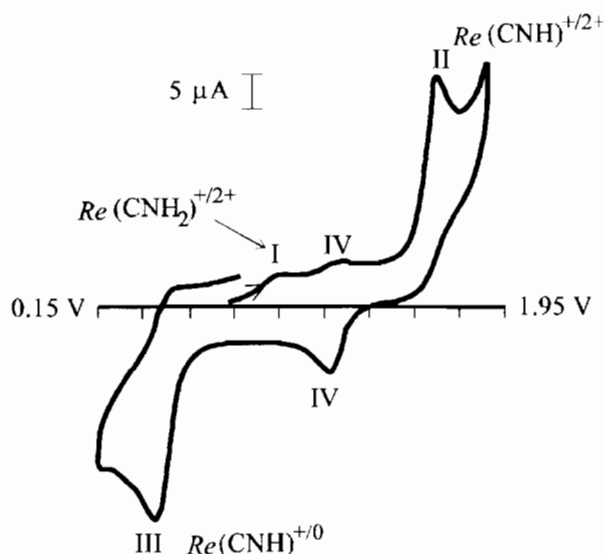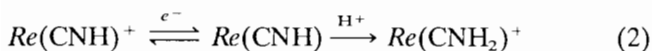
Fig. 3. Cyclic voltammogram recorded after the controlled potential electrolysis at wave I of a solution of *trans*-[ReCl(CNH₂)(dppe)₂][BF₄], in 0.2 mol dm⁻³ [NBu₄][BF₄]/NCMe, at a Pt-gauze electrode (scan rate = 200 mV s⁻¹; potential in V vs. SCE). Wave I is due to residual starting complex, whereas waves II and III are the anodic and cathodic waves, respectively, of $Re(CNH)^+$ generated along the electrolysis. Anodic wave IV is conceivably due to the oxidation of $Re(CN)$, formed by limited H⁺ dissociation from $Re(CNH)^+$, whereas the cathodic wave IV corresponds to the reduction of postulated $Re(CN)^+$ mainly derived from H⁺ dissociation from $Re(CNH)^{2+}$ generated at wave II. $Re = trans$-{ReCl(dppe)₂}.

according to Eq. (1), which consumes $Re(CNH)$ formed at wave (III) to regenerate the aminocarbyne complex (Eq. (2)).

$$Re(CNH)^+ \underset{}{\overset{e^-}{\rightleftarrows}} Re(CNH) \xrightarrow{H^+} Re(CNH_2)^+ \qquad (2)$$

(ii) The controlled potential electrolysis at the anodic wave (I) of the aminocarbyne complex forms, in high yield, $Re(CNH)^+$ (rose coloured solution), as indicated by the cyclic voltammogram (Fig. 3) run after such an electrolysis (waves II and III are the characteristic anodic and cathodic waves for that species). The measured number of electrons transferred per molecule of complex exceeds slightly the unity, possibly accounting to the further oxidation (at the anodic wave IV) (Fig. 3) of a product, possibly $Re(CN)$, derived, in a limited extent, from H⁺ dissociation of $Re(CNH)^+$ (see below).

(iii) The electrode process at the anodic wave (I) leads to proton dissociation as measured by potentiometric titration of the electrolyzed solution at the potential of that wave. A total of 2H⁺ has been titrated by using a ~1.3 mM NaOH solution in MeOH, but the titration curve presents two end-points, the first one conceivably corresponding to the titration of free H⁺ and the second one to that of $Re(CNH)^+$. The proton liberation was also consistent with the detection, by cyclic voltammetry (cathodic sweep) of the electro-

lyzed solution, of an irreversible and broad cathodic wave assigned to H⁺ reduction (see below).

The proton evolution at the anodic wave of $Re(CNH_2)^+$ agrees with the expected enhancement of the acidic character of the aminocarbyne ligand as a result of oxidation of the complex and parallels the anodically induced deprotonation reported for some aminocarbene complexes of Pd or Pt [6].

3.1.2. Second anodic wave

As explained above, the second anodic wave in the cyclic voltammogram of a solution of $Re(CNH_2)^+$ (wave II, Fig. 2) is in fact the first anodic wave of $Re(CNH)^+$ derived from the former complex at wave (I) according to reaction (1).

The oxidation of $Re(CNH)^+$ (wave II) involves the transfer of one electron and generates a product which is reversibly reduced at $E_{1/2}^{red} = 1.20$ V, as confirmed by the exhaustive controlled potential electrolysis at the anodic potential of wave (II). This electrolysis involves a single electron per molecule of complex and forms quantitatively a product (violet coloured solution) with the reversible cathodic cyclic voltammetric wave (IV).

The similarity between the cyclic voltammetric behaviour of $Re(CNH)^+$ at wave (II) with that of $Re(CNH_2)^+$ at wave (I) is evident (see Fig. 2), as well as the analogy between these two complexes with related ligands whose acidic character would be expected to increase upon oxidation. Therefore, the oxidation of $Re(CNH)^+$ at wave (II), by analogy, could also result in proton dissociation, according to reaction (3), to give $Re(CN)^+$ which would be the species reversibly reduced at wave (IV) ($E_{1/2}^{red} = 1.20$ V).

$$Re(CNH)^+ \underset{}{\overset{(II)}{\underset{-e^-}{\rightleftarrows}}} Re(CNH)^{2+} \longrightarrow Re(CN)^+ + H^+ \qquad (3)$$
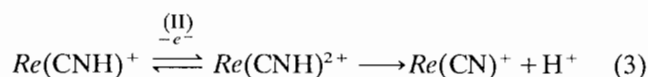
Attempts to isolate the postulated $Re(CN)^+$ complex from the electrolyzed solution have failed in view of its instability, thus precluding its direct characterization by the usual methods (however, see Section 5).

However, further indirect evidence can be presented to support that formulation, as follows.

(i) The two anodic processes at waves (I) and (II) (Eqs. (1) and (3)), as a whole, would correspond to an overall $-2e^-/-2H^+$ process (Eq. (4)) of conversion of the aminocarbyne into the cyanide ligand; this overall conversion has a precedent [10] in the formation of the related complexes *trans*-[MCl(CN)(dppe)₂] (M = Mo or W) from *trans*-[MCl(CNH₂)(dppe)₂].

$$Re(CNH_2)^+ \xrightarrow{-2e^-/-2H^+} Re(CN)^+ \qquad (4)$$
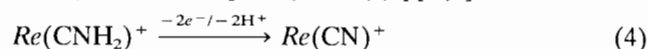
(ii) The proton liberation upon controlled potential electrolysis of a solution of $Re(CNH_2)^+$ at wave (II) has been detected by the cathodic sweep of the cyclic

voltammogram of the electrolyzed solution (broad and intense cathodic wave assigned to H^+ reduction, see below), as well as by its potentiometric titration (total of $\sim 2H^+$, although the essay is not entirely reliable due to the possible decomposition, along the titration, of the electrolysis product).

(iii) The product of the controlled potential electrolysis at wave (II) does *not* react with a strong base, as indicated by the maintenance of its reversible cathodic wave at $E_{1/2}^{red} = 1.20$ V (wave IV) upon addition of [NBu$_4$]OH (even in a fivefold molar excess). This agrees with the formulation of that product as a complex derived from the full deprotonation of the CNH_2 ligand, such as the postulated cyanide compound $Re(CN)^+$.

3.2. Cathodic behaviour

A solution of the aminocarbyne complex $Re(CNH_2)^+$ exhibits, by cyclic voltammetry, at a Pt electrode, an irreversible cathodic process at $E_p^{red} = -0.67$ V with generation, in part, of the hydrogen isocyanide compound $Re(CNH)$ detected by its typical reversible anodic wave at $E_{1/2}^{ox} = 0.40$ V (wave III). By replacing the Pt by a vitreous carbon working electrode, the $Re(CNH)$ complex is also generated upon a cathodic scan, but no defined cathodic wave is then observed, thus suggesting that proton reduction is occurring at the above-mentioned cathodic wave at -0.67 V which is clearly observed at a Pt electrode.

The presence of H^+ in solution would result from the slight acid dissociation, in neutral medium, of $Re(CNH_2)^+$ as accounted for by the detection, by cyclic voltammetry, during the anodic sweep, of the oxidation wave (III) of $Re(CNH)$, at 0.40 V, although with a rather weak current intensity (Fig. 2).

Therefore, the cathodic formation of $Re(CNH)$, involving reduction of liberated H^+ from $Re(CNH_2)^+$, could be explained by considering the resulting shift of the dissociation equilibrium of the latter complex as indicated by Eq. (5).

$$Re(CNH_2)^+ \rightleftharpoons$$
$$Re(CNH) + H^+ \xrightarrow{e^-/-H} Re(CNH) \quad (5)$$
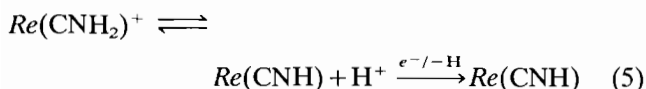
Moreover, a solution of $Re(CNH)$ exhibits, by cyclic voltammetry, at a Pt electrode, an irreversible cathodic process at $E_p^{red} \approx -0.70$ V, a value which is identical to that displayed by a solution of $Re(CNH_2)^+$ (see above). Replacement of a Pt by a vitreous carbon electrode results in a shift of the cathodic wave to a much lower potential (~ -2.0 V). The behaviour is similar to that detected for a solution of $Re(CNH_2)^+$ and also suggests that the cathodic wave at ~ -0.70 V (Pt electrode) corresponds to the reduction of H^+ dissociated from $Re(CNH)$. In agreement, no cathodic wave has been detected for the related organoisocyanide complexes *trans*-[ReCl(CNR)(dppe)$_2$] (R = alkyl or aryl)

[20]; in addition, if the reduction would occur at the complexes, it would be expected that $Re(CNH)$ would present the cathodic wave at a considerably lower potential than $Re(CNH_2)^+$, rather than at identical values.

Exhaustive controlled potential electrolysis, at a Pt-gauze electrode, of a solution of $Re(CNH_2)^+$ at the potential of the cathodic wave (H^+ reduction) observed at a Pt electrode, corresponds to the consumption of two Faradays per mole and evolution of H_2 which was detected by gas chromatography, in accord with Eq. (5) and the related behaviour observed for $Re(CNH)$. The presence, in solution, along the electrolysis, of $Re(CNH)$, although in low levels, was also detected by cyclic voltammetry.

The products formed at the cathodic process have not yet been fully elucidated, but an anodic wave, observed at $E_{1/2}^{ox} = -0.04$ V in the cyclic voltammograms run after the controlled potential electrolysis or following a cathodic sweep of a solution of $Re(CNH_2)^+$ or $Re(CNH)$, is conceivably associated to a complex cyanide product whose full characterization is under progress.

3.3. Digital simulation

The abovementioned reactions can be summarized by Scheme 1, whose anodic electrode processes have been further investigated by digital simulation of the cyclic voltammograms. Digital simulations were carried out as described in Section 2.

The results obtained for the kinetic constants and electrochemical parameters, by fitting the simulated voltammograms to the experimental ones, at different scan rates, are presented in Tables 1 and 2. The quality of the fittings can be observed in Figs. 4 and 5.

The study of the electrochemical behaviour of $Re(CNH_2)^+$ at various concentrations confirmed that the deprotonation steps are first order.

As can be seen from the values of the heterogeneous rate constants (k_{het}) in table 1, all the electrochemical processes involved in this scheme are quasi-reversible in the conditions of the experiments and the scan rates range.

The decomposition of postulated $ReCN^+$ was introduced as a result of the preliminary simulations made on this system and was also observed upon its synthesis by controlled potential electrolysis, thus precluding its isolation.

In the simulations, all the possible homogeneous redox reactions, between the redox pairs involved in Scheme 1, were also tested. As expected [21], most of these reactions have little or no influence on the shape of the voltammograms. Significant exceptions were the reactions involving the parent aminocarbyne complex, $Re(CNH_2)^+$, and the dioxidized isocyanide species,
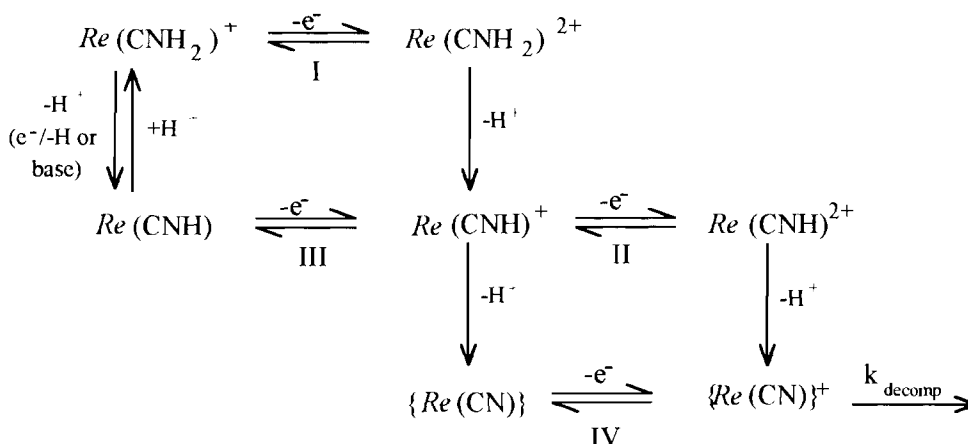
Scheme 1.

Table 1
Electrochemical parameters for the different redox couples involved in Scheme 1

	k_{het} (cm s^{-1})	$E°$ (V)
$Re(CNH_2)^+ \longrightarrow Re(CNH_2)^{2+} + e^-$	1.8×10^{-3}	0.84
$Re(CNH) \longrightarrow Re(CNH)^+ + e^-$	2.0×10^{-3}	0.45
$Re(CNH)^+ \longrightarrow Re(CNH)^{2+} + e^-$	1.0×10^{-2}	1.58
$\{Re(CN)\} \longrightarrow \{Re(CN)\}^+ + e^-$	1.0×10^{-2}	1.12

Table 2
Rate constants estimated by digital simulations for the chemical reactions involved in Scheme 1

	k_{dir} (s^{-1})	k_{inv} (ml mol^{-1} s^{-1})
$Re(CNH_2)^+ \rightleftharpoons Re(CNH) + H^+$	5×10^{-2}	8×10^6
$Re(CNH_2)^{2+} \rightleftharpoons Re(CNH)^+ + H^+$	>5	$-^a$
$Re(CNH)^+ \rightleftharpoons \{Re(CN)\} + H^+$	0.1	$-^a$
$Re(CNH)^{2+} \rightleftharpoons \{Re(CN)\}^+ + H^+$	2.	$-^a$
$\{Re(CN)\}^+ \longrightarrow$ unidentified products	0.3	

^{a}These constants are too small to be measured within the set of experimental conditions available.

$Re(CNH)^{2+}$, or the possible $Re(CN)^+$ complex. In these cases the shape of some of the waves was significantly altered, but only for kinetic constants above $\sim 1 \times 10^7$ ml mol^{-1} s^{-1} when the observed fittings were worse than those obtained if they were ignored.

However, in view of the low values we have obtained for the heterogeneous rate constants, and on the basis of the Marcus theory for electron transfer reactions [22], all the homogeneous redox reactions are expected to present low values for their rate constants, below those for which the shape of the voltammograms would be significantly altered.

As expected from the results, and mentioned above, the deprotonation of the aminocarbyne complex after oxidation, i.e. of $Re(CNH_2)^{2+}$, is fast. In fact, within
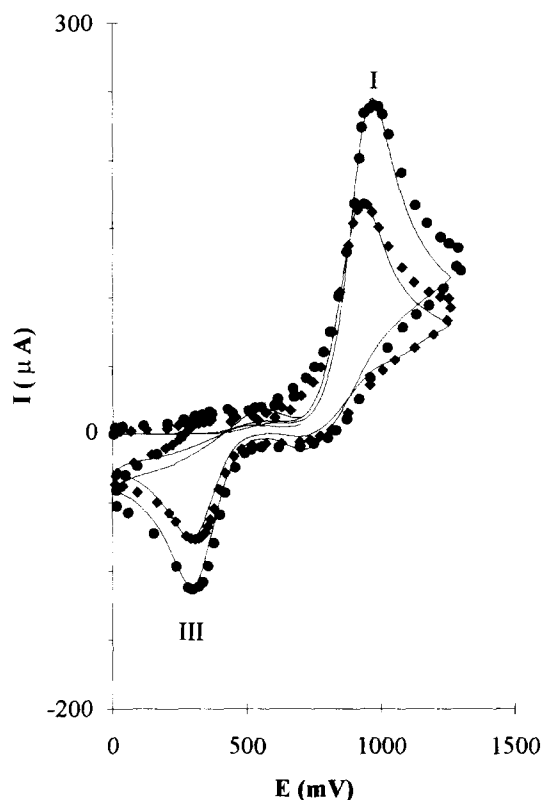

Fig. 4. Comparison of the experimental (symbols) and simulated (——) cyclic voltammograms for the first anodic wave, at a Pt wire electrode, of $Re(CNH_2)^+$ in 0.2 mol dm^{-3} [NBu$_4$][BF$_4$]/NCMe at a scan rate of 1000 (●) and 500 (♦) mV s^{-1}.

the studied scan rates range, it was only possible to conclude that the direct rate constant should be larger than 5 s^{-1}. This is consistent with the facts that the cathodic counterpart of the $Re(CNH_2)^+$ oxidation wave is not observed, and that the ratio between the intensities of the second (wave II) and the first (wave I) anodic peaks is approximately independent of the scan rate.

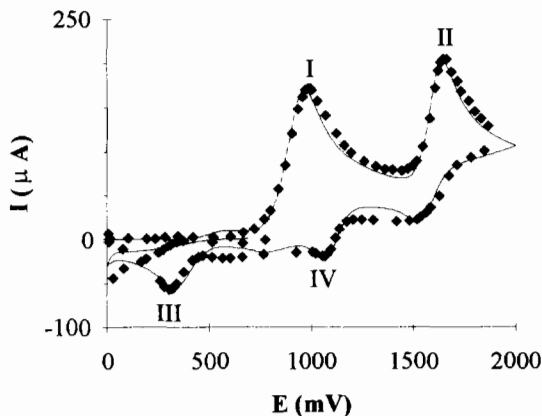However, the deprotonation of $Re(CNH)^{2+}$, formed at wave II from the oxidation of $Re(CNH)^+$, is con-

Fig. 5. Comparison of the experimental (♦) and simulated (——) cyclic voltammograms, at a Pt wire electrode, for a solution of $Re(CNH_2)^+$ in 0.2 mol dm^{-3} [NBu$_4$][BF$_4$]/NCMe at a scan rate of 500 mV s^{-1}.

$$Re(CNH_2)^+ \quad \underset{\text{I}}{\overset{-e^-}{\rightleftharpoons}} \quad Re(CNH_2)^{2+}$$

$$(K_a)\ -H^+ \downarrow\uparrow +H^+ \qquad\qquad (K_b)-H^+ \downarrow\uparrow +H^+$$

$$Re(CNH) \quad \underset{\text{III}}{\overset{-e^-}{\rightleftharpoons}} \quad Re(CNH)^+$$

$K_a = 0.05/(8 \times 10^6) = 6.3 \times 10^{-9}$ mmol ml^{-1} (dissociation constant for $Re(CNH_2)^+$), and using the standard potential obtained by simulation for the redox couples involved, we conclude[1] that the dissociation constant for $Re(CNH_2)^{2+}$, K_b, has the value of 25 mmol ml^{-1}. This confirms the statement above that the oxidized form, $Re(CNH_2)^{2+}$, has a much greater acidic character than $Re(CNH_2)^+$.

4. Final comments

The redox induced interconversion of the aminocarbyne (CNH$_2$) and the hydrogen isocyanide (CNH) species involves an increase of the acidity of the former promoted by oxidation (formation of CNH) or an increase of basicity of the latter group as a result of reduction of the oxidized forms of its complex (formation of CNH$_2$).

However, the cathodically induced conversion of CNH$_2$ into CNH apparently does not require electron transfer to the complex, by taking advantage of the easier reduction, at a less cathodic potential (at a Pt electrode), of H$^+$ (although present in low levels) formed by a reversible slight dissociation of CNH$_2$, with a resulting shift of this dissociation equilibrium towards the formation of the less protonated species.

Moreover, the hydrogen isocyanide ligand (CNH) appears to present a possible role in the interconversion between the aminocarbyne (CNH$_2$) and the cyano (CN) groups.

Nevertheless, we should also point out that, although some evidence suggests the formation of cyanide species, as discussed above, so far we have failed to fully characterize any of them from the electrolytic solutions (however, see Section 5), mainly as a result of their instability in the electrochemical medium. Although alternative interpretations could be postulated, in particular involving a redox induced CNH/NCH isomerization, they would present a greater complexity and
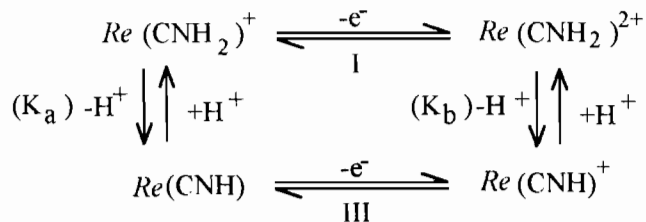
siderably slower, and its direct rate constant was estimated to be close to 2 s^{-1}.

Moreover, the rate of deprotonation of $Re(CNH)^+$ is even slower, in agreement with its lower charge. The aminocarbyne $Re(CNH_2)^+$ species also revealed some acidity in solution, since in all the voltammograms a small amount of $Re(CNH)$ was always found even before the anodic processes involving the parent compound took place.

Although all the deprotonation reactions were considered as equilibria in the calculations, only the reverse constant for the equilibrium between $Re(CNH_2)^+$ and $Re(CNH)$ was determined with a certain degree of confidence. This equilibrium is, in fact, important in the overall shape of the voltammograms, not only on account of the abovementioned dissociation, to a certain extent, of the $Re(CNH_2)^+$ species, but also because during the anodic sweep, after the cathodic wave (III) corresponding to the reduction of $Re(CNH)^+$, no significant anodic counterpart for that wave was observed (Fig. 1), indicating that the recombination of $Re(CNH)$ with a proton in solution is fast. All the other second order constants relating to the recombination of the various species with protons in solution seemed too small to be estimated in the time scale available in this set of experiments.

3.3.1. Acid dissociation constants

From the kinetic constants obtained for the acid/base equilibrium involving the $Re(CNH_2)^+$ complex it was possible to estimate the acid dissociation constant not only for this species but also for its oxidized form $Re(CNH_2)^{2+}$. In fact, by considering that the value of ΔG° for the thermodynamic cycle must be null, that

---

[1] This calculation is made taking into account that, for each thermochemical cycle, $\Delta G^\circ = 0$. If one considers the cycle in the scheme, the following relation can be obtained, in which $K_a = 6.3 \times 10^{-9}$ mmol ml^{-1} (see text), E° values are taken from Table 1, $F = 23061$ cal V^{-1} mol^{-1}, $R = 1.987$ cal mol^{-1} K^{-1} and $T = 298$ K, thus allowing to estimate the value of 25 mmol ml^{-1} for K_b: $0 = RT \ln(K_b/K_a) - F[E^\circ(Re(CNH_2)^{2+/+}) - E^\circ(Re(CNH)^{+/0})]$.

would be less satisfactory in accounting for the available experimental results.

5. Note added in proof

After the manuscript had been submitted for publication, we succeeded in isolating a product of the controlled potential electrolysis at wave II, which was analyzed by X-ray diffraction (by Professor A. Tiripicchio et al., University of Parma, Italy) and confirmed our proposed formulation, $\{Re(CN)\}^+$, as well as the first $CNH_2/CNH/CN$ interconversion at a metal centre (the details will be reported separately).

References

[1] F.R. Kreissl (ed.), *Transition Metal Carbyne Complexes*, NATO ASI Series C, Vol. 392, Kluwer, Dordrecht, Netherlands, 1993; G. Wilkinson, F.G.A. Stone and E.W. Abel (eds.), *Comprehensive Organometallic Chemistry*, Pergamon, New York, 1982.

[2] N.G. Connelly, in A.J.L. Pombeiro and J. McCleverty (eds.), *Molecular Electrochemistry of Inorganic, Bioinorganic and Organometallic Compounds*, NATO ASI Series C, Vol. 385, Kluwer, Dordrecht, Netherlands, 1993, p. 317, and refs. therein.

[3] M. Lange and D. Mansuy, *Tetrahedron Lett.*, 22 (1981) 2561.

[4] J.-P. Battioni, D. Lexa, D. Mansuy and J.-M. Savéant, *J. Am. Chem. Soc.*, 105 (1983) 207.

[5] C.P. Casey, L.D. Albin, M.C. Seaman and D.H. Evans, *J. Organomet. Chem.*, 155 (1978) C37.

[6] R. Bertani, M. Mozzon, R.A. Michelin, F. Benetollo, T.J. Castilho and A.J.L. Pombeiro, *Inorg. Chim. Acta, 189* (1991) 175.

[7] M.A.N.D.A. Lemos and A.J.L. Pombeiro, *J. Organomet. Chem., 356* (1988) C79.

[8] R. Bertani, M. Mozzon, R.A. Michelin, T.J. Castilho and A.J.L. Pombeiro, *J. Organomet. Chem., 431* (1992) 117.

[9] A.J.L. Pombeiro, D.L. Hughes, C.J. Pickett and R.L. Richards, *J. Chem. Soc., Chem. Commun.*, (1986) 246.

[10] (a) A. Hills, D.L. Hughes, C.J. Macdonald, M.Y. Mohammed and C.J. Pickett, *J. Chem. Soc., Dalton Trans.*, (1991) 121; (b) D.L. Hughes, S.K. Ibrahim, M. Moh'd Ali and C.J. Pickett, *J. Chem. Soc., Chem. Commun.*, (1994) 425.

[11] J.-G. Li, B.K. Burgess and J.L. Corbin, *Biochemistry, 21* (1982) 4393.

[12] G.L. Blackman, R.D. Brown, P.D. Godfrey and H.I. Gunn, *Nature (London), 261* (1976) 395, and refs. therein.

[13] (a) D.J. DeFrees, J.S. Binkley, M.J. Frisch and A.D. McLean, *J. Chem. Phys., 85* (1986) 5194; (b) M.P. Conrad and H.F. Schaeffer III, *Nature (London), 274* (1978) 456; (c) P.C. Burgers, J.L. Holmes and J.K. Terlouw, *J. Am. Chem. Soc., 106* (1984) 2762.

[14] W.P. Fehlhammer and M. Fritz, *Chem. Rev., 93* (1993) 1243.

[15] J. Joslin and D. Pletcher, *J. Electroanal. Chem., 49* (1974) 171.

[16] M.A.N.D.A. Lemos and A.J.L. Pombeiro, *Port. Electrochim. Acta, 10* (1992) 89.

[17] D. Britz, *Digital Simulation in Electrochemistry*, Springer, Berlin, 2nd edn., 1988.

[18] M.A.N.D.A. Lemos and A.J.L. Pombeiro, in A.J.L. Pombeiro and J. McCleverty (eds.), *Molecular Electrochemistry of Inorganic, Bioinorganic and Organometallic Compounds*, NATO ASI Series C, Vol. 385, Kluwer, Dordrecht, Netherlands, 1993, p. 477.

[19] J.E. Baur and R.M. Wightman, *J. Electroanal. Chem., 305* (1991) 73.

[20] A.J.L. Pombeiro, C.J. Pickett and R.L. Richards, *J. Organomet. Chem., 224* (1982) 285.

[21] D.H. Evans, *Chem. Rev., 90* (1990) 739.

[22] R.A. Marcus, *J. Chem. Phys., 43* (1965) 679; C.J. Schlesener, C. Amatore, J.K. Kochi, *J. Am. Chem. Soc., 106* (1984) 3567; C. Amatore, in M. Baizer and H. Lund (eds.), *Organic Electrochemistry*, Marcel Dekker, New York, 1991, Ch. 2.